A GUIDE TO ROUTINE SEISMIC MONITORING IN MINES

by

A J Mendecki, G van Aswegen and P Mountfort
ISS International Limited
P.O. Box 12063, Die Board, 7613, RSA
alexm@issi.co.za

in

This document is included as Chapter 9 of the publication, *A Handbook on Rock Engineering Practice for Tabular Hard Rock Mines*, *A J Jager and J A Ryder (eds.),* published by Creda Communications, Cape Town, 1999, on behalf of the Safety in Mines Research Advisory Committee to the Department of Minerals and Energy of South Africa.

**A Handbook on Rock Engineering Practice
for Tabular Hard Rock Mines**

Contents

1. Seismic Event, Seismicity and State of the Rockmass

Mining excavations induce elastic and then inelastic deformation within the surrounding rockmass. The potential energy accumulated in the rockmass may be unloaded or it may be released gradually or suddenly during the process of inelastic deformation.

A seismic event is a sudden inelastic deformation within a given volume of rock, i.e. a seismic source, that radiates detectable seismic waves. The amplitude and frequency of seismic waves radiated from such a source depend, in general, on the strength and state of stress of the rock, the size of the source of seismic radiation, and on the magnitude and the rate at which the rock is deformed during the fracturing process.

A seismic event is considered to be described quantitatively when apart from its timing, t, and location, $X = (x, y, z)$, at least two independent parameters pertaining to the seismic source namely, seismic moment, M, which measures coseismic inelastic deformation at the source and radiated seismic energy, E, or seismic moment and stress drop, $\Delta\sigma$, are determined reliably.
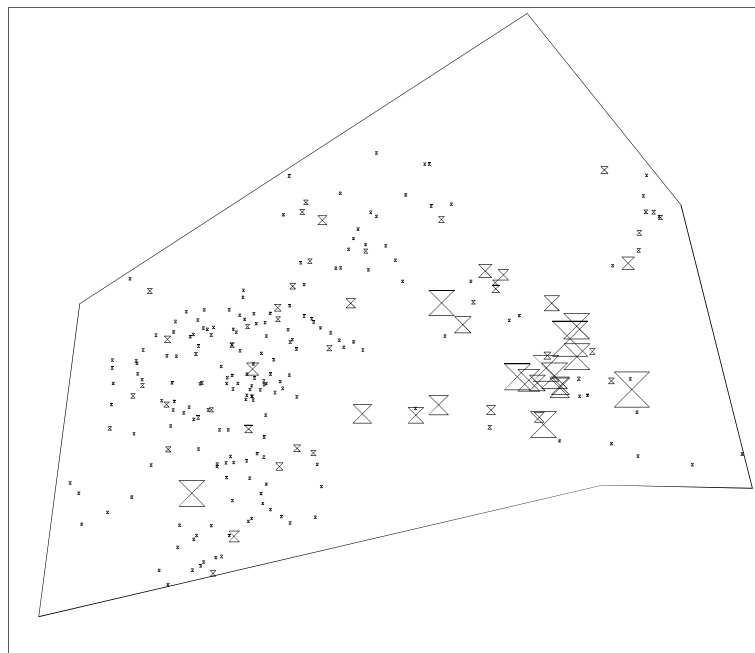
Figure 1 Apparent stresses of selected seismic events with equal local magnitudes *m ≈ 1.0* in a South African Gold Mine. The ratio of the highest to the lowest apparent stress on this figure is nearly 100.

Seismic waveforms do not provide direct information about the absolute stress, but mainly about the strain and stress release at the source. However, the source of a seismic event associated with a weaker geological feature or with a softer patch in the

rockmass yields more slowly under lower stress, and radiates less seismic energy per unit of inelastic coseismic deformation, than an equivalent source within strong and highly stressed rock. Therefore by comparing radiated seismic energies, or stress drops, of seismic events with similar moments one can gain insight into the stresses acting within the part of the rockmass affected by these events - see Figure 1.

A seismic system can measure only that portion of strains, stresses or rheology of the process which is associated with recorded seismic waves. The wider the frequency and amplitude range and the higher the throughput of the system, the more reliable and more relevant the measured values of these parameters become.

Having recorded and processed a number of seismic events within a given volume of interest ΔV over time Δt, one can then quantify the changes in the strain and stress regimes and in the rheological properties of the rockmass deformation associated with the seismic radiation.

This presents an opportunity to validate the results of numerical modelling of the design process. In numerical modelling, assumption of the same elastic constants within a given volume make strain, ε, and stress distribution equivalent, since $\sigma = constant \cdot \varepsilon$. However, seismically inferred stress and strain changes are independent. Seismic strain associated with seismic events in a given volume is proportional to seismic moments $\varepsilon_s \propto \Sigma M$, and seismic stress is proportional to the ratio of seismic energies to seismic moments $\sigma_s \propto \Sigma E / \Sigma M$. Thus contours of seismic strain and seismic stress may be qualitatively different, reflecting differences in stress regime and/or rockmass properties - see Figure 2 as an example. It is the difference between the modelled stress and/or strain distributions and the observed ones that need to be explained and reconciled with the design while mining.
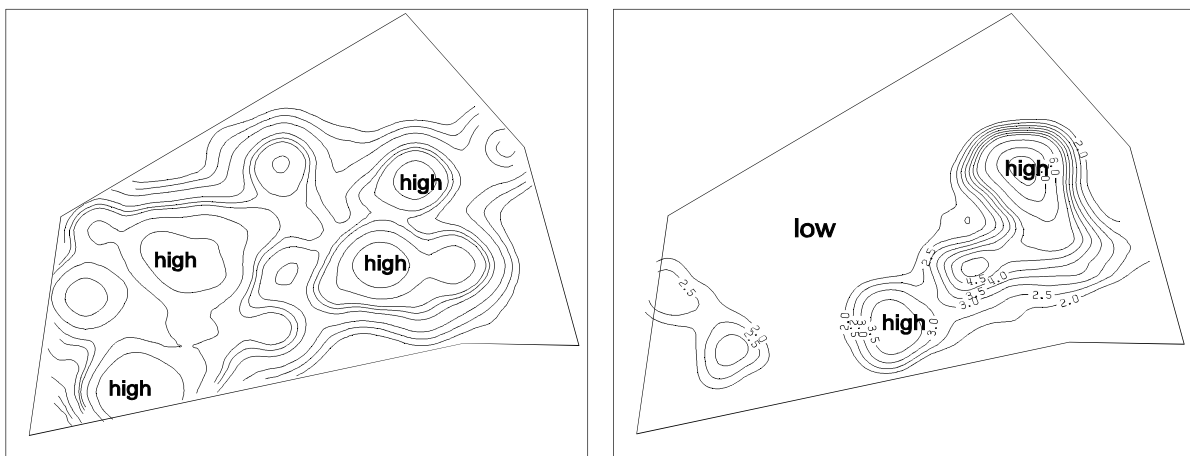
Figure 2 Contours of seismic strain (left) and seismic stress (right) for seismic events of all magnitudes in the area shown in Figure 1. Please note the qualitative difference between the distributions of seismic strains and stresses.

2. Objectives of Seismic Monitoring in Mines

In general, routine seismic monitoring in mines enables the quantification of exposure to seismicity and provides a logistical tool to guide the effort into prevention, control and prediction or warning of potential rockmass instabilities that could result in rockbursts. One can define the following specific objectives of monitoring the seismic response of the rockmass to mining:

- **Location of Potential Rockbursts**: To alert management by indicating the locations of potential rockbursts associated with intermediate or large seismic events and to assist in possible rescue operations - it is important then to monitor the locations of associated aftershocks.

- **Prevention**: To confirm some of the assumptions and parameters of the design process and to enable its continuity while mining. Specifically, it is important to confirm the critical assumptions of numerical modelling, i.e. assumptions to which stability parameters are sensitive, e.g. small changes in the orientation of and friction on a fault may considerably affect the predicted distribution of shear stresses acting on that structure. This assists in guiding preventative measures, e.g. corrections to the designed layout, sequence of mining, given rate of mining, support strategy, etc.

- **Control**: To detect spatio-temporal changes in seismic parameters, e.g. an increase in the number of intermediate and larger size events and in their time of day distribution, an increase in seismic diffusion, a degree of acceleration in seismic deformation and/or a decrease in seismically inferred stress - and relate these changes to the stability of deformation within the volume of interest. This would facilitate and guide control measures, e.g. managed workers exposure to seismicity at different times of day, a temporary slowdown or suspension and then resumption of mining in a given area and/or the timing and desirable location of preconditioning and triggering blasts.

- **Warnings**: To detect unexpected strong changes in the spatial and/or temporal behaviour of seismic parameters, or certain defined characteristic patterns that could lead to dynamic instabilities affecting working places. This would facilitate warnings to manage the exposure to potential rockbursts.

- **Back-analysis:** To improve the efficiency of both the design and the monitoring processes. Specifically important is thorough seismic and numerical modelling back-analysis of large instabilities even if they did not result in loss of life or in considerable damage. Back analysis of seismic rockmass behaviour associated with pillars, backfill, different mining layouts, rates and ways of excavating, etc, is an important tool in the quest for safer and more productive mining. It is desirable then to maintain the database of seismicity, i.e. times, locations, magnitudes, seismic moments, radiated energies, sizes and stress drops for all seismic events recorded. In addition, the

availability of waveforms of the seismic events recorded a few months prior to large events and rockbursts and located within a few source diameters of that event would assist in back analysis and research.

A quantitative description of seismic events and seismicity is considered necessary, although not sufficient, in achieving the above objectives.

3.   Location of Seismic Events

The location of a seismic event is assumed to be a point within the seismic source that triggered the set of seismic sites used to locate it. The interpretation of location, if accurate, depends on the nature of the rupture process at the source - if a slow or weak rupture starts at a certain point, the closest site(s) may record waves radiated from that very point while others may only record waves generated later in the rupture process by a higher stress drop patch of the same source. One needs to be specific in determining the arrival times if the location of rupture initiation is sought, otherwise the location will be a statistical average of different parts of the same source.

A reasonably accurate location is important for the following reasons:

•   to indicate the location of potential rockbursts;
•   all subsequent seismological processing, e.g. seismic source parameter and attenuation or velocity inversion, depends on location;
•   all subsequent interpretation of individual events depends on location, e.g. events far from active mining, close to a shaft or, in general, in places not predicted by numerical modelling, may raise concern;
•   all subsequent interpretation of seismicity, e.g. clustering and specifically localization around planes, migration, spatio-temporal gradients of seismic parameters and other patterns are judged by their location and timing.

Location error depends on the accuracy of the data. Table 1 lists the major aspects of the data and their minimum precision required for accurate location.

The location depends also on the numerical procedure adopted to solve the system of nonlinear site equations. The denser the network and the more accurate the data, the smaller is the influence of the numerical procedure. With high quality data from at least 5 sites of reasonable configuration, the location error may be reduced to less than 3% of the average hypocentral distance (AHD) of the sites used.

In the case of the velocity model not being known adequately, or if velocities change significantly with time, one can attempt to improve the location by the arrival time difference method, also known as 'master event' location or relative location. This procedure requires an accurately located master event (e.g. blast), in the proximity of the event to be relocated, that has reliable arrival times at sites used in the relocation procedure. It is inherently assumed here that the velocities of the seismic waves from the master event to the sites and those from the target event are the same. Since this is

not always the case, it is important that the two events should be close to each other; less than 10% of average hypocentral distance would be a good rule of thumb.

Table 1

Parameters Affecting Location Accuracy *Seismic site = the set of sensors with the same co-ordinates*	Recommended Minimum Precision
common time among seismic sites in the network	500μs
arrivals of P and/or S-waves at site	500μs or one sample
P and/or S-wave velocity model	7.5%
site coordinates	1m
sensors orientation at site, used to constrain the location by direction(s) or asimuth(s) of recorded waveforms; also used in seismic moment tensor determination	5 degrees
number of seismic sites	at least 5
the distribution of sites with respect to the position of the event to be located, e.g. as measured by the normalised orthogonality between straight ray paths from the hypocentre to the sites, *QC*: $$QC = 0.3873\sqrt{ns}\left[\det (C)\right]^{1/3}, \quad \text{where}$$ $$C = \begin{vmatrix} \sum \cos^2\alpha_i & \sum \cos\alpha_i \cdot \cos\beta_i & \sum \cos\alpha_i \cdot \cos\gamma_i \\ \sum \cos\alpha_i \cdot \cos\beta_i & \sum \cos^2\beta_i & \sum \cos\beta_i \cdot \cos\gamma_i \\ \sum \cos\alpha_i \cdot \cos\gamma_i & \sum \cos\beta_i \cdot \cos\gamma_i & \sum \cos^2\gamma_i \end{vmatrix}$$ and α_i, β_i, γ_i are directional angles between the hypocentre and the i-th site; $\sum$ runs over the number of sites, *ns*.	0.3

Since the source of a seismic event has a finite size, the attainable location accuracy of all seismic events in a given area should be within the typical size of an event of that magnitude which defines the sensitivity of the seismic network for that area, i.e. the minimum moment-magnitude, m_{min}, above which the system records all events with sufficient signal to noise ratio (SNR). The table below gives the recommended location accuracy for different network sensitivities associated with different objectives of monitoring. Approximate source sizes are quoted for reference.

Table 2

Objective of Monitoring	Location	Prevention		Control		Warnings	
Network sensitivity (m_{min})	1.0	0.5	0.0	-0.5	-1.0	-1.5	-2.0
Desired minimum location accuracy [m]	100	75	40	20	15	10	5
Approximate source sizes [m] at stress drops between 0.1 to 0.5 MPa	65-110	35-65	20-35	12-20	6-12	4-6	2-4

4. Quantification of Seismic Sources

Seismic events can routinely be quantified by the following parameters derived from recorded waveforms:

- time of the event, t
- location, $X = x, y, z$
- seismic moment, M, and its tensor which defines the overall direction of principal stresses acting at the source and the nature of the coseismic strain change in terms of its isotropic and deviatoric components
- radiated seismic energy, E, and/or seismic stress drop $\Delta\sigma$
- characteristic size of the event, l
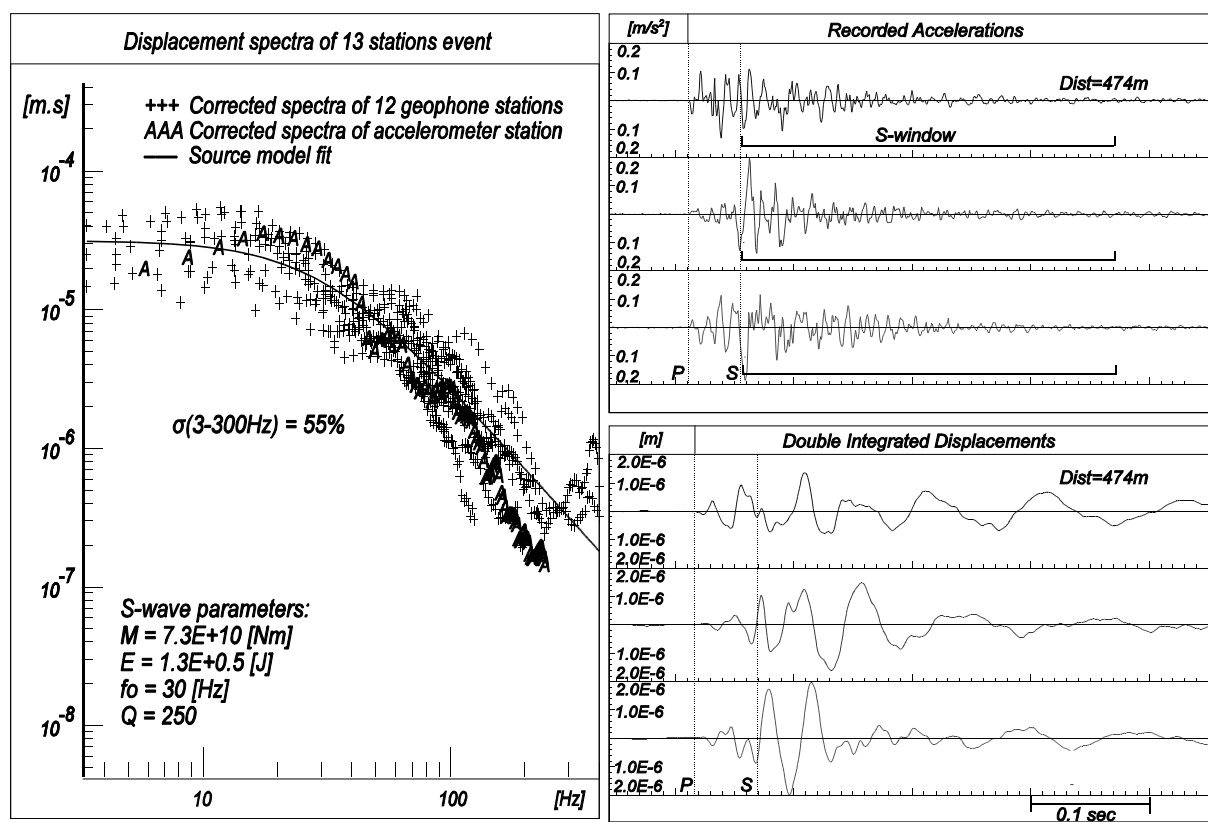
Figure 3 *Left* shows the stacked instrument, distance and Q-corrected S-wave spectra derived from waveforms recorded at 13 sites associated with a seismic event of $m = 1.1$. Uncertainty, as measured by standard error σ, is calculated in the frequency range 3-300Hz. Three-component waveforms of recorded accelerations with marked S-windows for spectral calculations and double integrated displacements, are shown on the *right*.

The routine estimates of seismic moments and radiated seismic energies from waveforms are relatively inaccurate, with uncertainties, as measured from the scatter of processed data around the model, from 50% for well behaved waveforms to over 100% for complex ones (Figure 3). However, the variation in radiated seismic energy (or stress drop) of seismic events with similar moments occurring in different stress and/or strain regimes at the same mine is considerably greater than the uncertainty in

measurements and the error propagation in processing - see Figure 1. Thus, while these uncertainties influence the resolution obtainable negatively, they should not prevent the quantitative interpretation and comparison of seismic strain and stress changes between different time intervals and/or between different areas covered by the same seismic system.

Seismicity is defined here as a number of seismic events, occurring within a given volume, ΔV, over a certain time, Δt. Seismicity can be quantified using the following four largely independent quantities:

- average time between events, $\bar{t}$,
- average distance, including source sizes, between consecutive events, $\bar{X}$,
- sum of seismic moments, ΣM, and
- sum of radiated energies, ΣE.

From these four basic quantities one can derive a number of parameters i.e. seismic strain ε_s, its rate $\dot{\varepsilon}_s$, seismic stress σ_s, relative stress σ_r, seismic stiffness K_s, seismic viscosity η_s, seismic relaxation time τ_s, seismic Deborah number De_s, seismic diffusivity D_s or d_s and seismic Schmidt number Sc_s, that describe the statistical properties of coseismic deformation and associated changes in the strain rate, stress and rheology of the process - see Glossary of Terms for general descriptions. Table 3 lists the major aspects of data used in source parameter calculations and the minimum precision required for reasonable results.

Table 3

Parameter Affecting Source Parameter Calculation	Recommended Minimum Precision/Value

calibrated, resonance free frequency range ±3dB
  m_{max} - the maximum magnitude event to be measured
  m_{min} - the magnitude that defines sensitivity of the network
	f_{min} = $0,5f_0(m_{max})$
	f_{max} = $5f_0(m_{min})$

geophone natural frequency	5%
geophone damping factor	5%
geophone sensitivity	5%
accelerometer sensitivity	5%
number of sites	5 x 3 component each, or 3 x 3 comp. plus 6 single comp.
location accuracy	5% of AHD
hypocentral distance	$> \lambda$ = wave velocity / f_0
SNR = A_{max}/*pretrigger noise level*	10
P and S wave velocities	7.5%
P and S wave attenuation & scattering Q	20%
rock density at the source	10%

window length for source parameters
  $T(A_{max})$ - period associated with maximum amplitude on
  velocity waveforms
	$4{\cdot}T(A_{max})$

Uncertainties between the observed displacement spectra, corrected by the average radiation pattern, and the model.	75%

5. Seismic Hazard and Seismic Safety

In general seismic hazard relates to the potential for strong ground motion resulting from the occurrence of seismic events. Seismic hazard is defined as the probability of occurrence of an input, i.e. seismic event or ground motion, equal to or exceeding a specified level, within a given period of time.

The general procedure followed in evaluating hazard includes the determination of the volumes that produce seismicity, estimating the recurrence times of seismic events of different magnitudes and, taking into account the local attenuation of ground motion and site effects, computing the probability of exceeding a given level of ground motion for different time intervals. The results may be presented as a table of probability of each level of ground motion for a given site or as contours of different levels of ground motion at a given level of probability. Seismic hazard estimates in mines are frequently limited to probabilities of occurrence, or recurrence times, of seismic events above certain magnitudes $\bar{t}(\geq m)$, so the relative exposure to seismicity and seismic risk could be quantified.
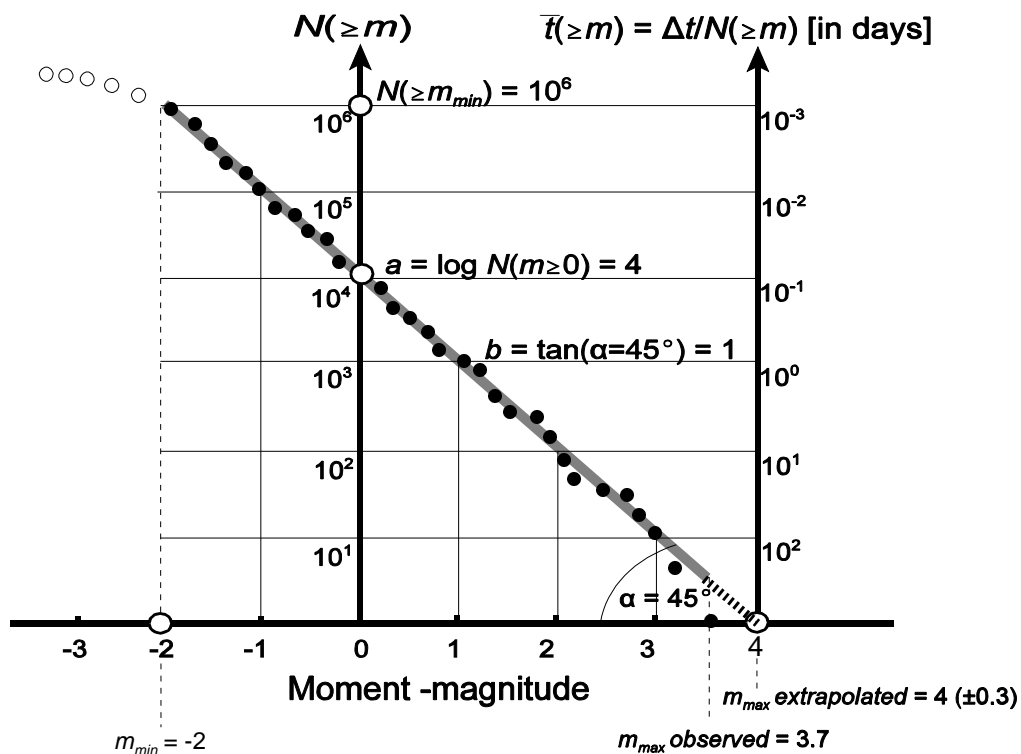
Figure 4 An illustrative plot of cumulative frequency-magnitude with m_{min} = -2, a = 4 and b = 1 for the volume ΔV over the time period Δt = 1000 days. Open dots below m_{min} = -2 denote data points below the network's sensitivity that should not be used in parameter estimation.

The probabilistic recurrence times can be derived from different modifications of the empirical Gutenberg-Richter relation describing the frequency-magnitude distribution of small and intermediate size earthquakes,

$$\log N(\geq m) = a - bm,$$

where $N(\geq m)$ is the expected number of events not smaller than magnitude m, and a, b are constant - see Figure 4. The Gutenberg-Richter relation implies a power law distribution i.e. the absence of a characteristic size, and as a consequence, puts no limit on the maximum earthquake size. Thus if the distribution of large earthquakes is also a power law, then it must have an exponent that is larger than that for smaller ones.

The mean recurrence times can be calculated as $\bar{t}(\geq m) = \Delta t / N(\geq m)$, where Δt is the period of observation. The one largest seismic event, called here m_{max}, would have a magnitude that corresponds to $N(\geq m_{max}) = 1$, or $\log 1 = a - bm_{max} = 0$, thus $m_{max} = a/b$, or

$$m_{max} = m_{min} + (1/b)\log N(\geq m_{min}), \text{ with uncertainty } \delta m_{max} = \pm 0.3/b.$$

Parameter a measures the overall occurrence rate and, for the same b, scales with the rate of rockmass deformation $\dot{\varepsilon}$ as $a = \log \dot{\varepsilon} + constant$. The parameter b is controlled by the distribution of events between the higher- and lower-magnitude ranges and, for large and well distributed data sets, can be estimated from $b = 0.43(\bar{m} - m_{min})^{-1}$ with uncertainty $\delta b = \pm b/\sqrt{n}$, where $\bar{m}$ is the mean of the observed magnitudes and n is the number of observations. Both parameters influence derived recurrence times, therefore it is essential that their values and variances be determined accurately. The basic assumptions made when calculating the probabilistic recurrence times are that $N(\geq m_{max}) = 1$ and the parameters a and b do not change significantly with time and within the selected volume ΔV.

The estimated number of seismic events within the magnitude range m_1 and m_2, where $m_1 < m_2 \leq m_{max}$, is $N(m_1 \leq m \leq m_2) = N(\geq m_1) - N(\geq m_2)$, and the cumulative moment release, ΣM, by all these events can be estimated from

$$\Sigma M = b \cdot 10^{a+9.1}(10^{m_2(1.5-b)} - 10^{m_1(1.5-b)})/(1.5-b), \quad \text{for } b < 1.5.$$

In the long term the sum of seismic moments is proportional to the volume mined, V_m, $\Sigma M \simeq GV_m$. Thus, for a given V_m, the higher the values a and b of the Gutenberg-Richter relation the lower the m_{max}.

The specific model of the frequency-magnitude relation and the numerical procedures used in its parameter estimation should account for the upper limit of possible maximum magnitude in the area of interest, slow temporal changes in b, and for the fact that magnitudes are not continuous but discrete grouped quantities determined, in mines, with accuracy of 0.2 units on average.

If one assumes that the time of rupture of larger events is controlled by strong and highly stressed areas within the volume ΔV, the recurrence time $\bar{t}(\geq m)$ should then be calculated on the basis of frequency - magnitude data selected from these areas only,

as determined by the contours of energy index or seismic stress and/or modelled stress, instead of from the entire volume.

The most significant deviations of observations from the frequency-magnitude relation are those at the largest observed magnitudes, since they may influence the expected recurrence time for the maximum magnitude event. In general, recurrence times beyond the time span of the data set Δt should be treated with caution.

In addition, it is useful to know the distribution of actual recurrence times about the estimated mean. Given the mean, the type of distribution, the standard deviation of the observations and the time of occurrence of the last event, either cumulative probability, i.e. the probability that an event would already have happened, or future conditional probability may be estimated. Failing that, one can evaluate the best estimate of the empirical probability P_T that a given volume ΔV will produce an event of magnitude greater than m within a specific time T after the preceding event of this size. Given the latest n observed recurrence intervals $\bar{t}\,(\geq m)$, of which n_T are smaller than or equal to T,

$$P_T = (n_T + 1)/(n + 2), \text{ with uncertainty } \delta P_T = \pm 2\sqrt{P_T(1 - P_T)/(n + 3)}.$$

For larger data sets, δP_T approximates the 95% confidence interval. For example, consider a sequence of the last 15 recurrence intervals in days, for events with $m \geq 3.0$ in one of the mining areas in South Africa: 86, 33, 118, 58, 31, 107, 61, 77, 10, 17, 8, 13, 4, 26, 4. Then, the empirical probability that this area will produce an event with $m \geq 3.0$ within, say, $T = 90$ days of the preceding one is $P_{90} = 0.82$ with $\delta P_{90} = \pm 0.18$, which could be considered reasonably significant. For the same data set, $P_{30} = 0.47$ with $\delta P_{30} = \pm 0.23$ would not be considered significant.

In general the b-value is influenced by the following characteristics of the geomechanical system under consideration:
- the stiffness, i.e. the ability to resist deformation with increasing stress
- the level of stress
- the rockmass heterogeneity.

The stiffer the system the higher the b-value. This observation does not contradict reports on decreasing b-value with increasing stress, since there is a general loss of stiffness with increasing stress during a strain hardening regime. In the absence of a significant tectonic stress, intermediate and large seismic events usually occur after considerable mining has taken place in the area, degrading the stiffness of the system.

The rock mass heterogeneity is defined by the spatial distribution of sizes and distances between strong and/or stressed and weak and/or destressed patches of rock where seismic sources may nucleate and be stopped. In general, for the same stiffness, an increase in rock heterogeneity results in a higher b-value, since it is more likely that an initiated rupture be stopped by a soft or hard patch before growing into a larger event.
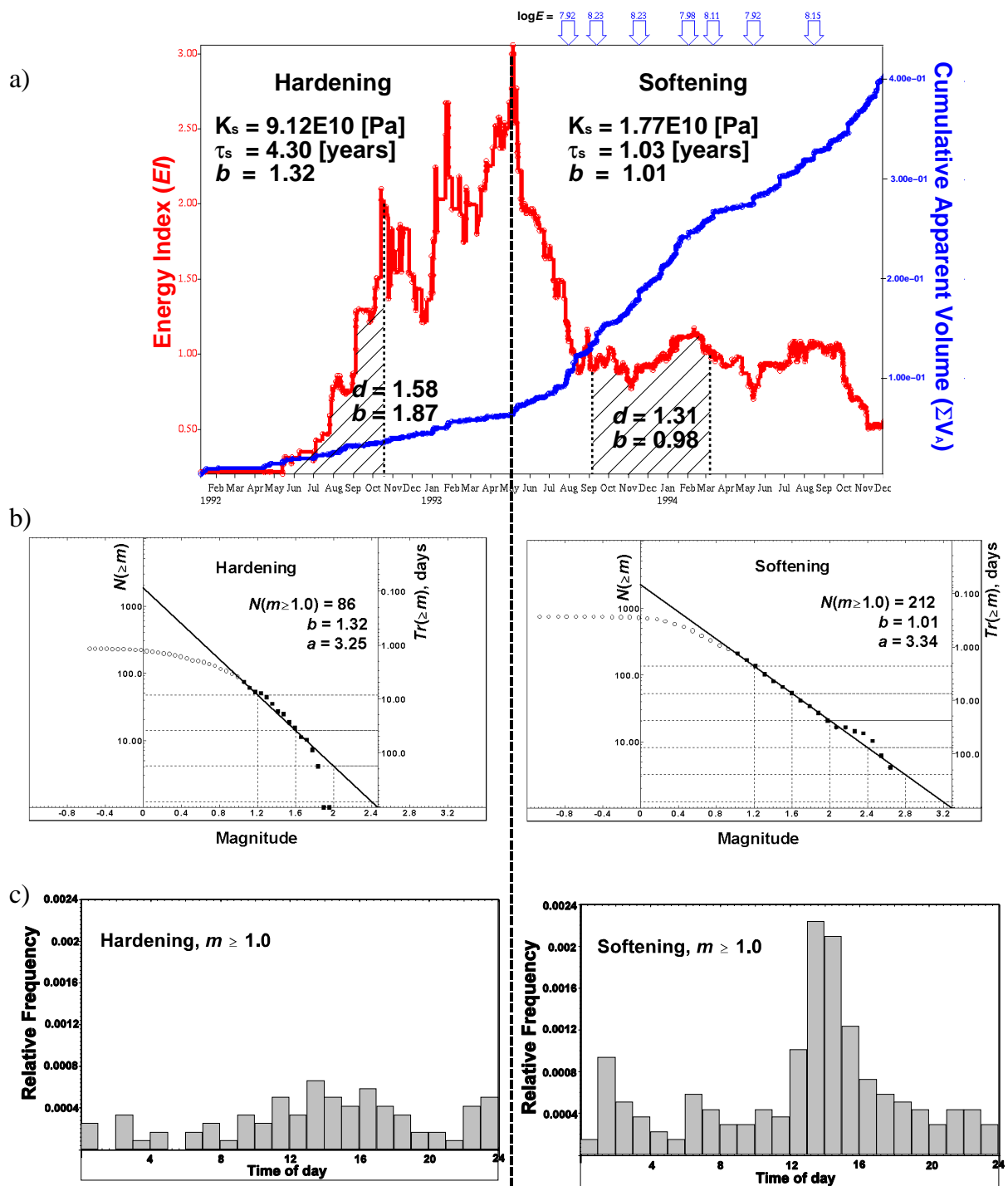
Figure 5(a) Time history of cumulative apparent volume, ΣV_A, and energy index, EI, for the seismicity associated with pillar mining within the volume $\Delta V = 5.12E7m^3$. Note that all large seismic events, $\log E > 7.5$, occurred after the pillar had lost the ability to maintain stress. Note also the differences in d-value (slope of the E-M relation) and in the b-value between two six-month periods, indicated by shading, of similar average energy index EI but considerable difference in stiffness.

Figure 5(b) The cumulative frequency-magnitude distributions for the period of January '92 to May '93 (hardening) and June '93 to December '94 (softening); note the characteristic misfit (the lack of larger events) between the data and the model during the overall hardening regime; note also a considerably higher hazard associated with larger seismic events during the softening period.

Figure 5(c) The time-of-day distributions of seismic events with $m \geq 1.0$ for the hardening and softening periods; note that hazard for $m \geq 1.0$ at 23h00 until 01h00 and at 10h00 and 12h00 is higher during hardening.

Rockmass subjected to mining is strongly influenced by excavations, pillars, induced fracture zones, and associated changes in stress. These induced heterogenieties influence the stiffness and the stress regimes of the system and thus the activity rate, size of the larger observed events and the b-value. For example, an introduction of strike stabilizing pillars in the West Rand Region in 1980 and, recently, the sequential grid layout, both reduced the size of the largest events experienced compared to the traditional longwall mining. Figure 5 shows cumulative apparent volume vs energy index, size and the time-of-day distributions derived from seismic data recorded during shaft pillar extraction. Note the softening of the pillar during May 1993 manifested by persistent decrease in energy index *EI* associated with an increase in the rate of seismic deformation and associated changes in the size and time distributions.

Similarly the d-value defining the slope of the log*E* vs log*M* straight line fit, called the *E-M* relation, tends to correlate with the system stiffness - the stiffer the system the steeper the line and the higher the d-values – see Figure 6. The *E-M* relation for the stiff system does not extend far into the large moment domain since it does not produce large events until its stiffness is degraded and the d-value drops. For a given slope an increase in the c-value of the *E-M* relation reflects an increase in stress - the apparent stress of a typical event with $M = 1$Nm, or $m = -6$, would be $\sigma_A(M = 1) = rigidity * 10^c$.
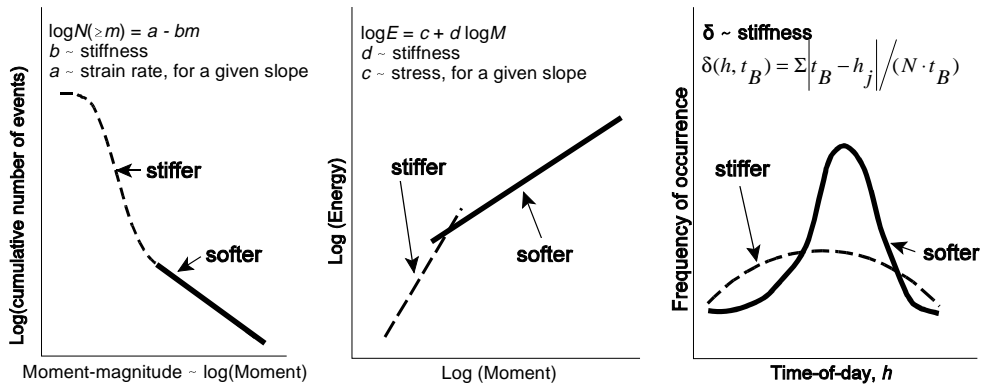
Figure 6 An illustration of a cumulative frequency-magnitude plot of a mixed data set over a limited period of time (left). Events associated with a stiffer system (broken line) and with a softer system (solid line) frequently have different slopes. On a log Energy vs log Moment plot (centre) the same applies. Intermediate and larger events associated with softer systems tend to occur within a few hours of blasting time, t_B, while a stiffer system responds moderately but with larger statistical dispersion, as measured by the normalised standard deviation δ, (right).

The observed data sets of mining related seismicity frequently exhibit fairly complex behaviour. The frequency-magnitude distributions of seismic events associated directly with tunnel development, or mining excavations and those related to geological features of different sizes may have different forms, and when superimposed may affect the estimated recurrence times of larger events – see Figure 6. In addition, the relatively subjective choice of volume(s) of interest, the

range of spatial and the degree of temporal correlation of seismic activity and the availability and quality of data may also influence the results. Therefore many data sets could be considered anomalous, having either a peculiar *b*-value, i.e. outside $0.5 < b < 1.5$, and/or strongly deviating from the Gutenberg-Richter model. In such case it is important to determine the physical factors affecting the distribution and ensure that the interpretation is offered in the context of the specifics of the data set.

Seismic hazard derived from the size distribution of seismic events may not be adequate to quantify and to manage the exposure to seismicity, due to the differences in time of day distribution of intermediate and large events associated with different mining scenarios, see Figure 5 as an example. In general stiffer systems/layouts are characterised by the lower m_{max} but by the time-of-day distribution with larger statistical dispersion in relation to the time of blasting, thus they are less time-predictable, while softer systems have larger m_{max} but they trigger or induce most events during the few hours after blasting.

If $\bar{t}(\geq m, t-t_B) = (t-t_B)/N(\geq m, t-t_B)$, is the recurrence time of events with magnitude not smaller than *m* at the time *t* after the time of blasting t_B, then the probability of having an event of that size in a small time interval $t + \Delta t$ is approximately $P(\geq m, t+\Delta t) \simeq \Delta t / \bar{t}(\geq m, t-t_B)$.

Seismic exposure at a given hour of day, *SSE(h)*, averaged over Δt can be estimated by the product of the average frequency of potentially damaging events $N(\geq m, h) / \Delta t = 1 / \bar{t}(\geq m, h)$, and the average number of people exposed at that time, *npe(h)*

$$SSE(h) = npe(h) / \bar{t}(\geq m, h).$$

The daily *SSE* can then be taken as a sum

$$SSE = \sum_{h=1}^{24} npe(h) / \bar{t}(\geq m, h).$$

6. General Guidelines for Interpretation

Mining excavations induce considerable gradients in strains and stresses and in their rates, which the rockmass continuously reduces, mainly by inelastic deformation. This process is strongly time dependent, e.g. the relaxation time changes over a few orders of magnitude within a short distance from the excavation faces. Such strong spatial and temporal gradients are conducive to the development of excess stresses which, if not diffused, result in large and/or strong seismic events.

Analysis and interpretation of seismic events:
The magnitude and the strength of the event: The occurrence of a larger, in terms of its seismic moment, and stronger, in terms of its stress release, seismic event indicates the potential for rockbursting in that area. The higher the stress release, for a given magnitude, the higher the hazard.

The occurrence of an unexpected event: The occurrence of a larger seismic event not predicted spatially and/or temporally by numerical modelling should raise concern.

Event mechanism: The seismic moment tensor solution, if available, may assist in validating the results of numerical modelling by correlating the expected and the observed directions of principal stresses in the area and the expected and the observed isotropic and deviatoric components of the coseismic strain change.

Analysis of seismicity in space - contouring. The main objective of spatial analysis of seismicity is to delineate the areas/volumes of concern from a stability point of view. Frequently larger seismic events occur or are initiated at "spots" of significant spatial stress and/or strain related gradients.

Spatial or 2D contours of stress related parameters is the simplest, and in many cases, a very effective, way of delineating sites of increased rockburst hazard. Contours of Energy Index (*EI*) are sensitive indicators of stress variation.

Routine spatial analysis can be improved if seismic stress and strain indicators are viewed simultaneously. Frequently larger events occur at sites of high strain gradients, characterised by high stress. The situation can be recognised where contours of, say, seismic strain, seismic viscosity or seismic Deborah number are closely spaced and, at the same time, superimposed contours of *EI* show high values.

The time span over which such analyses are done depends on the nature of the rockmass behaviour and the scale of the analysis. It is advisable to limit the time period over which the strain related parameter is contoured to not more than the seismic relaxation time. For the stress related parameter a shorter period is required since the cumulative strain over a period of time is to be compared with the present state of stress.

Analysis of seismicity in time. The main objective of temporal analysis of seismicity is to establish and, if possible, to quantify the imminence of potential instability. Frequently larger seismic events are preceded by an increase in stress followed by its decrease and accelerated coseismic deformation - see Figure 7. Consequently one may observe a decrease in seismic viscosity and an increase in diffusivity, d_s, resulting in a sharp drop in seismic Schmidt number before instability. Since the dynamics of the preparation and nucleation of rockmass instabilities is not well understood, unexpected strong changes in seismic parameters in any direction should raise immediate concerns - see Figure 8 as an example.

Cumulative apparent volume (ΣV_A): The slope of the ΣV_A curve sensitively reflects changes in strain rate. Accelerating deformation over a period of time is an indication of unstable rockmass deformation. Larger events stand out as jumps in the cumulative curve without distorting the scale, as is the case with cumulative seismic energies or moments. In addition its time history does not have to be treated with statistical smoothing. It is therefore a useful reference curve on a time history plot when

comparing the behaviour of other parameters requiring filtering procedures. The time history of seismic viscosity similarly measures the nature of the seismic rock deformation and a decrease in the value of this parameter reflects softening. It is sensitive to the size of the moving time window used.

It is recommended that seismic strain related parameters in spatial and/or temporal analysis be compared with volume mined, V_m.
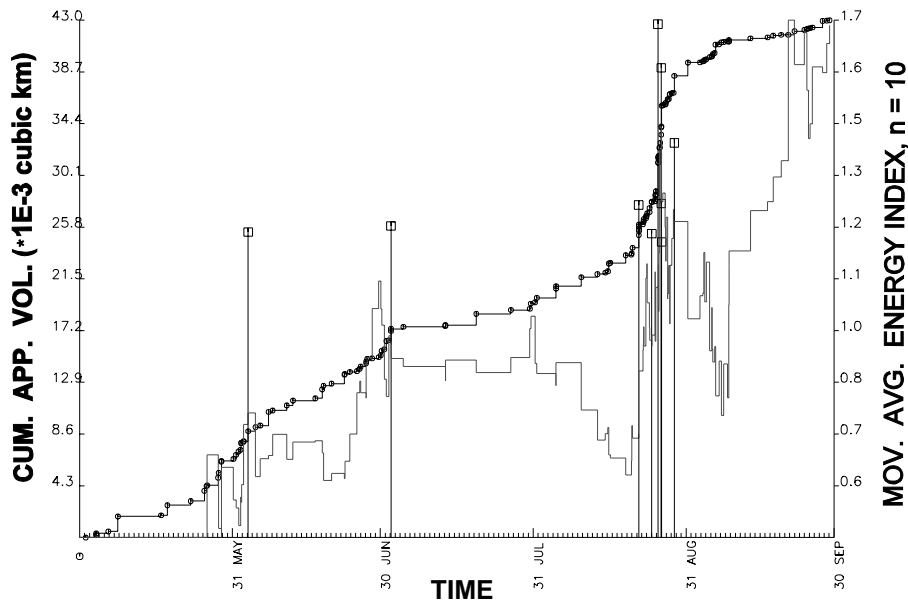
Figure 7 Cumulative apparent volume (thick dotted line) and moving average energy index (thin dashed line) versus time for mining area surrounding a dyke in Welkom, South Africa. The largest seismic events with $m \geq 1.7$ are marked by square capped vertical lines. (Reproduced with kind permission from Kluwer Academic Publishers)

Energy Index: A moving median *EI* has been proven a reliable and sensitive indicator of stress variation both in space and time. Using a linear scale, a time plot of *EI* does, by definition, emphasise above average values. If the purpose is more general, i.e. to monitor variation above and below average, log(*EI*) is the recommended parameter.
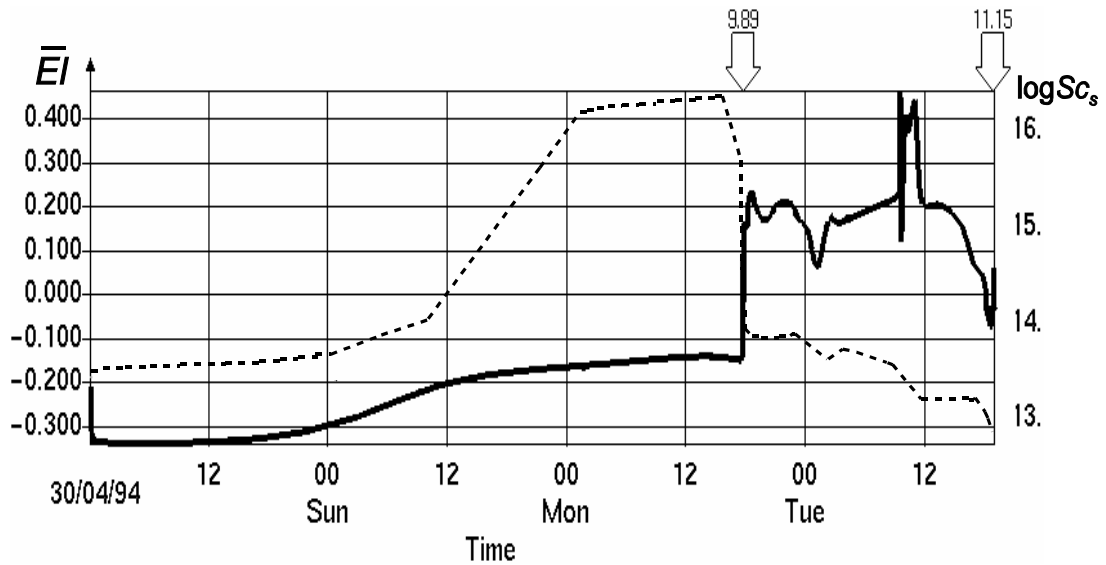
Figure 8 Time history of a moving median energy index, $\overline{EI}$, for the 90 hours preceding a magnitude $m = 4$ event ($\log E = 11.15$) in a South African gold mine. An increase in $\overline{EI}$ associated with the $\log E = 9.89$ on Monday late afternoon had been maintained for approximately 18 hours when another sudden increase occurred (late Tuesday morning). At that point the decision to evacuate the area was taken by the management on the advice of the mine seismologist. The dotted line shows the behaviour of the seismic Schmidt number.

Activity rate: Since very small events do not contribute significantly to seismic strain and cannot significantly change the state of stress, their occurrence may be missed by analyses which concentrate on overall strain rate and average stress level. Specific attention to activity rate could help to recognise anomalous patterns in rockmass behaviour. Sudden unexpected increase in activity rate should raise concern. For meaningful interpretation of activity rate, the seismic network sensitivity must remain constant.

Spatio-temporal parameters:
Seismic Schmidt number measures the spatio-temporal complexity of seismicity - the lower the seismic Schmidt number the less stable the seismic deformation. By encompassing the four independent seismicity parameters of (ΣE, ΣM, $\overline{X}$ and $\bar{t}$), seismic Schmidt number is the single most useful indicator of potential instability. It is found practical to use the log of the parameter in time history analyses - see Figure 8.

Local clustering of seismic activity in time and/or in space can relatively easily be accounted for when computing average values of different parameters quantifying seismicity. Let Ω represent the parameter of interest, say:
$\Omega = \varepsilon_s, \sigma_s, K_s, \eta_s, D_s (\Delta V, \Delta t)$, then the local space and/or time clustering of Ω can be expressed as

$$C(\Omega; \overline{X}, \bar{t}) = \Omega/(\overline{X} \cdot \bar{t}),$$

where $\bar{X}$ and/or $\bar{t}$ would cater for the local spatial and/or temporal clustering of seismic activity - see Figure 9 as an example.
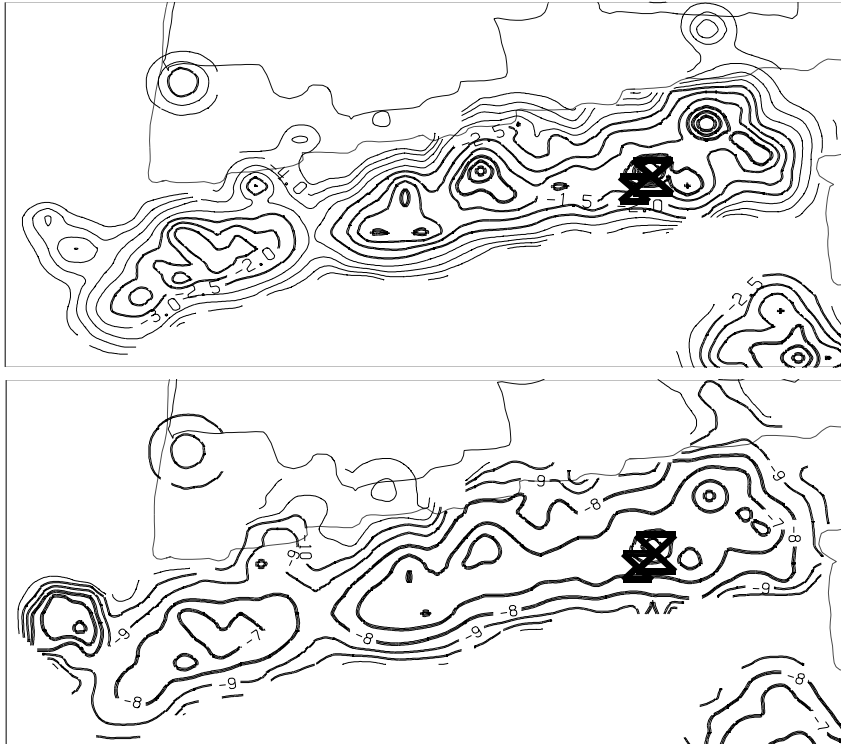
Figure 9 In the *top* figure contours of log D_s of one month's data of seismic response to longwall mining in a South African gold mine are shown. One can distinguish at least four areas of high gradient with D_s as high as 0,5 to 1 m²/s. One of these areas attracted two larger seismic events, marked by the hourglass symbols, a day later. The *bottom* figure shows contours of $C(D_S;\bar{t}) = D_S/\bar{t}$ in [m²/s/s], where seismic diffusivity is divided by the local average time (over grid size) between seismic events $\bar{t}$. The two larger events which subsequently occurred located in the area of the maximum $D_s/\bar{t}$.

Differential maps. The objective of differential maps is to delineate the areas or volumes of significant changes in the parameter of interest over time. It may help to identify hot spots, i.e. areas/volumes of undesirable rock mass response to mining, for more detailed time domain stability analysis.

Differential maps are presented as contour lines in 2D or surfaces in 3D of equal difference in a given parameter between two periods of time, say Δt_2 and Δt_1, over the same area or volume of interest. For routine analysis it is advisable that Δt_2 and Δt_1 be equal and consecutive. The grid spacing, hence the spatial resolution of the map, is a function of location accuracy and the network's sensitivity - the lower m_{min} the better the spatial coverage by small events.

Differential maps may be used to reconcile the results of numerical modelling with those of quantitative seismic monitoring, i.e. the expected percentage changes in stress and/or strain related parameters predicted by time step modelling can be compared qualitatively and quantitatively with percentage change in the relevant observed seismic parameters. Back-analysis of stable and unstable cases would generally assist in validating the procedure before routine use.

7. Characteristics of Seismic Monitoring Systems

The transducers, data acquisition hardware and processing software which comprise seismic monitoring systems can best be characterised in terms of the amplitudes and frequencies of the ground motion which they can faithfully represent, and the rate at which events may be recorded and processed.

Frequency bandwidth and dynamic range. The magnitudes which may practically be monitored in mines range from -4, which are the smallest from which one can routinely extract useful information about the state of the rock mass, to 5, which are the largest events experienced.

The predominant frequency radiated from the source, called the corner frequency of the seismic event, is related to the seismic moment and stress drop of the event by $f_0 = 1815 \sqrt[3]{\Delta\sigma/M}$ for the S-wave in hard rock. Figure 10 illustrates this relation, where the width of the lines is due to variation with rock type. The most information on coseismic strain change is contained in the lower frequencies, and on coseismic stress change in the higher frequencies, of seismic radiation. Thus a frequency bandwidth of at least $f_0/2$ to $5f_0$ is recommended to measure theses changes with useful accuracy.
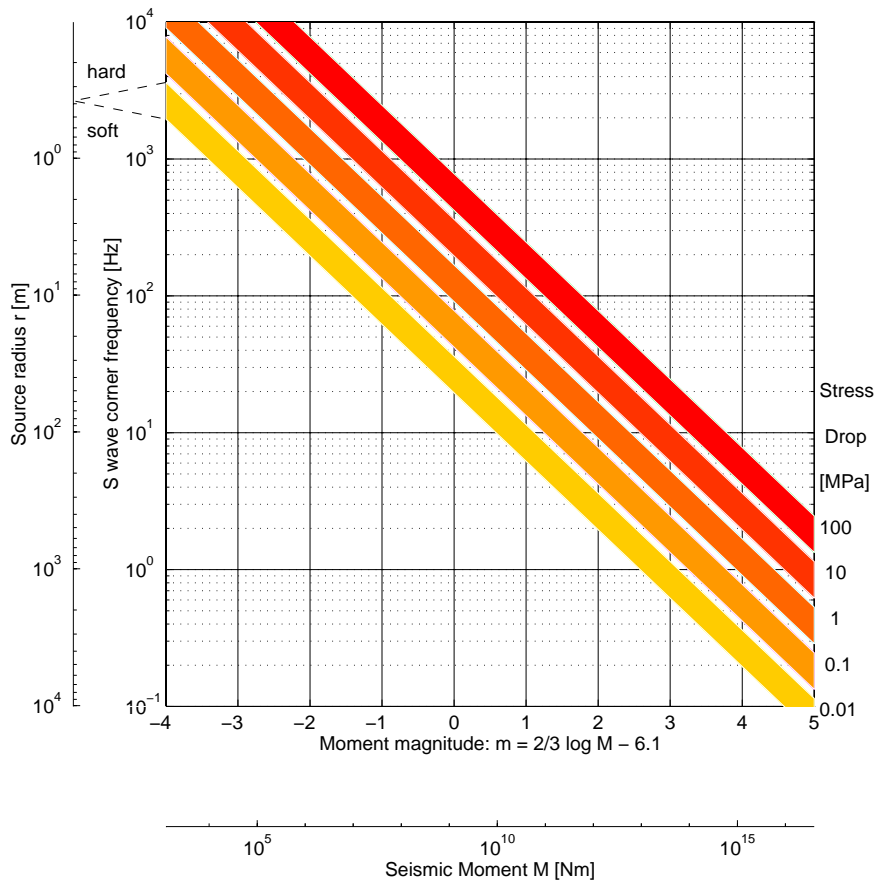
Figure 10   Expected source radius *r* and S-wave corner frequency f_0
as a function of seismic moment for a range of stress drops.
(Reproduced with kind permission from Kluwer Academic Publishers)

Since the amount of energy radiated by events within our range of interest, from
magnitude -4 to +5, varies by at least 10 orders of magnitude, and the energy received
by each sensor varies with the inverse square of distance from the source over a wide
range of distances, it can be seen that a very wide range of ground motion amplitude
must be accommodated. Allowing only for geometrical spreading to account for
reduction of ground motion with distance, then for each event the product of distance
from the source *R*, and peak ground velocity v_{max} is a constant. In hard rock it is
related to the source parameters by

$$Rv_{max} = 7 \times 10^{-9} \sqrt[3]{\Delta\sigma^2 M}, \text{ see Figure 11.}$$
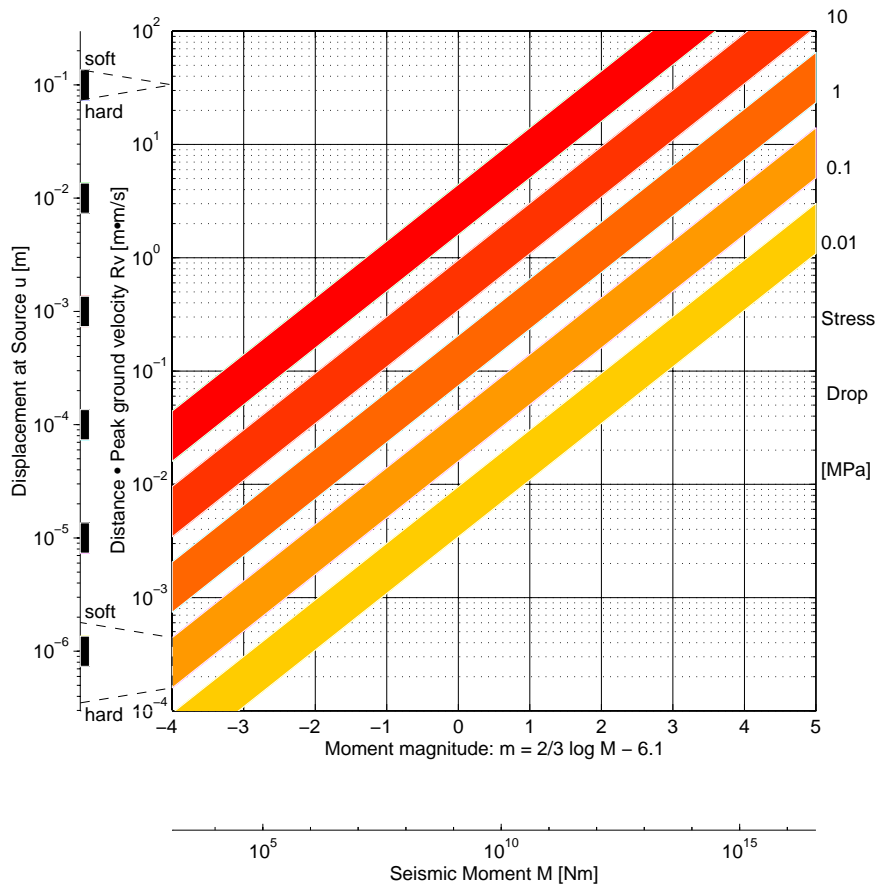
Figure 11 The product of distance from the source and the far field peak ground velocity, Rv_{max}, and displacement at the source, u, plotted as a function of moment for a range of stress drops. The width of the lines represents the variations due to a range of rock types. (Reproduced with kind permission from Kluwer Academic Publishers)

The sensitivity of a network may be gauged from peak amplitudes on recorded data, the distance from the source at which they were measured and the energy radiated from the source. A cumulative frequency-amplitude plot, analogous to the frequency-magnitude plot in Figure 4, allows the determination of the smallest amplitude which is reliably recorded on a particular network, with given noise levels and trigger settings. Similarly, the decay of amplitude with distance, which is always greater than the 1/distance from geometrical spreading, may be determined from the recorded data, as may dependence on seismic moment. Combining these quantities yields a maximum distance at which a given magnitude event may be detected. Such a relation, from data recorded on a South African gold mine, is shown in Figure 12, for ground velocity and acceleration.
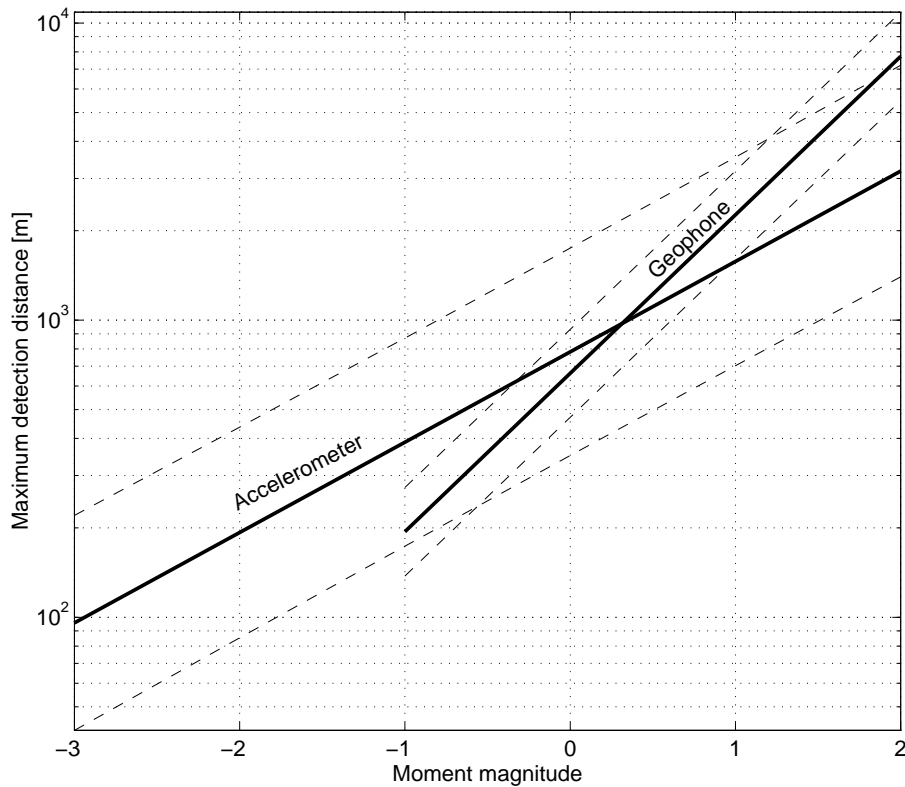
Figure 12 Minimum detectable distance as a function of magnitude, measured in a South African gold mine. The accelerometer shows much less variation with magnitude than the geophone, as expected. These values depend on environmental noise, trigger levels set by the operator, wave attenuation through the rock, and other factors which vary from network to network.

The dynamic range of a system is defined as the ratio of the maximum signal level that may be recorded to the noise level when no signal is present. This ratio is usually expressed in decibels:

$$R = 20 \log (S/N) \ [\text{dB}]$$

The dynamic range of commonly used sensors is illustrated in Figure 13. The system should have approximately 120 dB dynamic range or more if it is to take full advantage of sensor capability. This range may also be expressed as 1 000 000 : 1 or 20 bits, since this is the number of binary weighted digits necessary to specify integer values in this range.

The resolution, or number of significant bits, on the other hand, depends on the ratio of signal to noise plus distortion in the presence of signal. The sensors commonly used in mines generate at least 0.1% distortion at large amplitudes, which is 1000 : 1 or 60 dB or 10 bits signal to distortion ratio. Thus the system should have at least 10 bits resolution at all points within its 20 bit dynamic range.

Since noise power is usually evenly distributed over the whole recorded frequency band, the noise level may be reduced, and hence the dynamic range increased, by reducing the bandwidth of the recording to match that of the signal. Decimation is the process of filtering a recording to remove unwanted frequencies and resampling at a lower rate to match the reduced bandwidth. For the case of evenly distributed noise power, 3 dB dynamic range is gained for each halving of the bandwidth.

The latest technology, known as sigma-delta, delta-sigma, oversampling or noise-shaping, for producing digitisers with high dynamic range and high resolution makes extreme use of this concept. The signal is digitised at a high sampling rate with low resolution, typically 1 bit, in such a way that the majority of the noise induced by the quantisation is at very high frequencies. These data are then decimated to the required sampling rate, typically by a factor of 256, by which stage the dynamic range is very good. The simplicity of the 1-bit modulator front end usually results in excellent resolution as well.
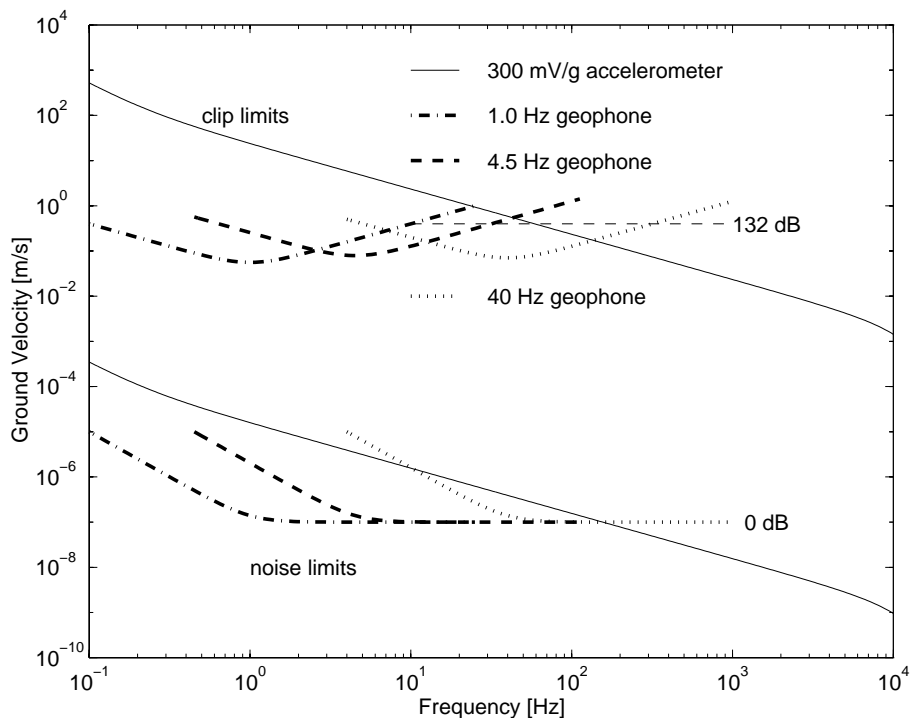
Figure 13 Sensitivity and dynamic range of sensors commonly used in mine seismic systems. The region between the limits represents the usable range for each instrument. The geophone's greater sensitivity up to several hundred hertz is clearly shown, as is the loss of dynamic range due to displacement clipping below these frequencies. A data acquisition system dynamic range of 132 dB with its quantization noise matching the expected ground noise of 10^{-7} m/s is illustrated. (Reproduced with kind permission from Kluwer Academic Publishers)

Sensors. Two types of sensor which provide coverage within the frequency range of Figure 10 are miniature geophones and piezoelectric accelerometers. The amplitudes of ground velocity which they can measure are shown between the noise limits and

clip limits in Figure 13 as a function of frequency. Choice of sensor type and other logistical and physical network parameters are summarised in Table 4, for different application domains, based on the following considerations:

• Geophones are ideal for sparse networks, where sensors are separated by distances of the order of 1 km on average. Their sensitivity allows them to record relatively distant events, and there is little chance of a large event being near enough to more than one sensor to cause clipping. Geophones do not exhibit particularly high levels of linearity, 0.2% distortion at 18 mm/s being the typical specification.

• Piezoelectric accelerometers are ideal for dense networks where sensors are separated by of the order of 100 m on average. The high frequencies to which they are sensitive are attenuated by propagation through the rock, so many sensors must be close to the active source volumes. Their comparative insensitivity to low frequencies ensures that very large events occurring within the same volume will not cause clipping. Accelerometers exhibit fairly large nonlinearities, distortion generally being specified at 1 % or 2 % near full amplitude. Transverse sensitivity can be as high as 5 %.

• By comparing Figures 10 and 13, it may be seen that neither miniature geophones nor piezoelectric accelerometers cover the low frequencies generated by the larger magnitude lower stress drop events. For these cases it is useful to add at least one short period earthquake monitoring instrument to a mine network in the form of a 1 Hz geophone or strong motion force balance accelerometer which provides for the recovery of moment for the largest events.

Sensor installation. Sensors should be installed in boreholes which extend beyond the heavily fractured rock surrounding the excavation. The sensor should be installed in grout that provides good coupling to the rock, and the borehole filled to avoid the trapping of acoustic energy. For this purpose grout should have similar acoustic impedance, i.e. the product of density and propagation velocity, to the rock. These precautions are necessary for accurate measurement of higher frequency signal components.

The sensors should be installed with a known orientation. For lower frequency geophones this is important as proper operation depends on being closely aligned, within 5 degrees, of the vertical or horizontal. In addition knowledge of the orientation of the sensors provides additional information which is useful for location and vital for the calculation of the moment tensor.

Where a sensor is placed on the surface, on soil rather than bedrock, a concrete mount may be used provided that the radius of the mount is less than $\frac{1}{9}$ of the wavelength at the highest frequency to be recorded.

Table 4

Application	Recommended Minimum System Characteristics
Regional mining, monitoring of several operations on a regional basis, larger seismic events, $m_{min} \geq 0$ over longer distances, 1 – 30 km	Low Frequency: 1 Hz - 500 Hz Sensor density: 5 sites within 5 km of the source Sensors: Geophones/Force Balance Accelerometers Dynamic range: 120 dB Resolution at all signal levels: 12 bits Event rate: 1 - 100 events per day Sustained event rate: 25 per hour Communication rate: 1.2 kb/s Communication method: single twisted pair and/or radio
Mine or shaft-wide monitoring $m_{min} \geq -1$ and at 300 m to 5 km	Medium frequency: 1 Hz - 2 kHz Sensor density: 5 sites within 1 km of the source Sensors: Geophones/Piezoelectric Accelerometers Dynamic range: 120 dB Resolution at all signal levels: 10 bits Event rate: 100 - 1000 events per day Sustained event rate: 250 per hour Communication rate: 9.6 kb/s Communication method: dual twisted pair and/or optical fibre
Microseismic monitoring, $m_{min} \geq -3$ and at 100 m to 1 km	Wide frequency band: 1Hz - 10 kHz Sensor density: 5 sites within 300 m from the source Sensors: Piezoelectric Accelerometers Dynamic range: 110 dB Resolution at all signal levels: 10 bits Event rate: 1000 - 10 000 events per day Sustained event rate: 2500 per hour Communication rate: 115kb/s Communication method: copper cable and/or optical fibre

System performance. The throughput of a system in terms of the rate at which events can be recorded and processed must generally be considered on three different time scales. The shortest time scale defines the *burst* rate, and is a reflection of how much storage is available for events immediately after triggering - this is temporary storage only and should accommodate at least 10 events to allow for fluctuation in time between events and seismogram duration. Second is the *sustained* rate, determined by the speed with which data may be transferred to permanent storage and automatically processed - see Table 4. Third is the *daily* rate, which is largely governed by the pattern of mining activity. For example, if blasting occurs once a day and generates 90% of the seismic activity within 2 hours, the daily event tally will be only those events which could be transferred at the sustained rate during those two hours. Additional local storage, up to hundreds of events, can usefully extend this time.

If a frequency-magnitude relation for the volume of interest is known or inferred and a desired network sensitivity in terms of m_{min} has been decided, then an estimate may be made of the required communication rate, R[bits/s].

Given $N(\geq m_{min})$ for $\Delta t = 1$ day, and assuming:

- 10 000 seconds per day in which to transmit the events, following the 90/10 time distribution above,
- 2000 samples per seismogram and 6 bytes per triaxial sample, and
- 10 bits per byte including protocol overheads yields

$$R = [N(\geq m_{min}) + n_r] \cdot 12 \text{ [bits/s]}$$

per triaxial sensor site, where n_r is the expected number of rejected waveforms per site per day due to environmental noise and events of less than m_{min} which cause the network to trigger.

8. Limitations of Seismic Monitoring and Future Development

Waveforms of seismic events contain newly created information about the state of the rockmass at and in the vicinity of their sources at the time of their occurrence. The information becomes useful only once extracted and translated into parameters relevant to associated changes in strain and stress and/or into characteristics of the complex dynamics of seismic rockmass response to mining.

The fundamental limitation of seismic monitoring is our limited understanding of the radiation processes at seismic sources and inability to recover all useful information from waveforms. The same applies to seismic processes leading to rockbursts where certain recognisable spatio-temporal patterns exist only over limited time period after which a dynamical reorganisation occurs that leads to the appearance of a new but still temporary pattern of events. The nature of the processes responsible for this complex dynamics is not as yet understood and it severely limits the predictability of rockmass response to mining by either the numerical modelling or seismic monitoring techniques. In addition the sparseness of seismic sites, the use of geophones insensitive to high frequency, as opposed to accelerometers, and the low bandwidth of the communication network, limits the sensitivity of the system and thus the information about the rockmass behaviour in space and in time.

In today's practice of quantitative seismology in mines, only waveforms with well-developed P and S wave signatures, sufficient signal to noise ratio, low complexity, negligible near and intermediate field terms of source radiation and weak site effects are being processed routinely. This exacerbates the sparseness of spatial and temporal information about the state of the rockmass.

The following are the main directions in future research and development to realize the stated objectives of monitoring seismic rockmass response to mining:

- One needs to increase the sensitivity i.e. the frequency range, amplitude range and the throughput of seismic monitoring systems, to account for a greater portion of stress and strain changes due to mining and to gain information from the parts of the rockmass otherwise considered inactive and from the
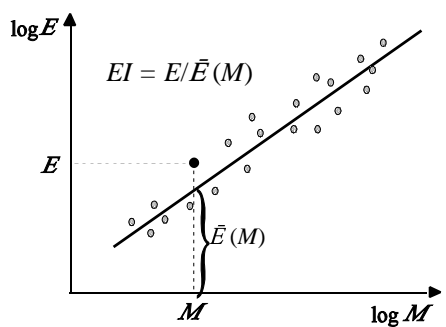
periods of time otherwise considered quiet. In addition, use of non-seismic sensors, e.g. strain-, stress-, creep-meters; convergence measurements, etc, would assist in monitoring changes in the relatively slowly varying so called static stress field which are thought to be an important triggering mechanism implying the existence of longer range correlations before failure. This is specifically important when monitoring the stability of geological structures subjected, in addition, to transient loads associated with seismic waves from nearby seismic events.
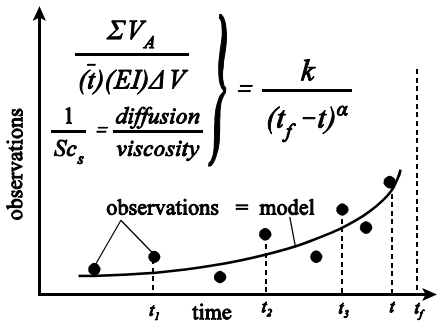
- There is a need to reliably describe the complexity of the source of a seismic event not only by its time, location, radiated seismic energy, seismic moment, and size but in addition by its shape, orientation, rupture directivity and duration, and to quantify seismicity by parameters pertaining to changes in stress, strain and rheology of seismic deformation processes. Such a quantification would allow the integration of results of seismic monitoring with numerical rheological models that capture the underlying dynamics. Developed models should be capable of reconstructing the main patterns of seismicity, i.e. size distribution, time distribution, clustering and migration, facilitating the design-as-you-mine process whereby the difference in modelled and observed rockmass behaviour could be explained and reconciled while mining.

- Quantitative stability analyses are not yet routine practice at all mines. They are currently done on the basis of qualitative interpretation of quantitative data provided by modern seismic systems, e.g. by analysing changes in parameters describing the size and time distribution of seismic events and their relation to stress and stiffness, and/or by monitoring the rate of seismic deformation and of seismically inferred stress change. Procedures need to be developed to formalize this qualitative process, to quantify the potential for rockmass instability that may result in rockbursts and to correlate it with the specifics of mine layouts, rates of mining, way of excavating etc., for a given quantified geological setting.

- The recent development in 'time-to-failure', that takes into account rates of change in strain, stress and the complexity of seismic rockmass behaviour, may provide a tool not only to quantify the imminence of potential instability in the short term and to make the process more objective, but also to correlate with and eventually to integrate this type of development into numerical modelling.

- By analysing only 'good quality' waveforms of 'well behaved' seismic events one is utilising only a fraction, less than 1%, of the time the rockmass responds seismically to mining. There is a considerable information loss by not recording and analysing waveforms, associated with convolved fracturing, complex seismic events and nonstochastic rockmass noise, that constitutes a legitimate seismic rockmass response to mining. Such noise, or rather fluctuations, play a creative role in processes of self-organisation, pattern

formation and coherency and can alter the system in fundamental ways. Consequently the models of rockmass behaviour close to excavations should allow for the influence of such fluctuations. It is therefore important to develop methodologies, technologies and logistics for *continuous*, in addition to intermittent, monitoring of seismic rockmass response close to the excavation faces, where sensors are positioned in the near-field at the centre of the volume of interest *where the action is*, as opposed to being outside in the far field. The processing and analyses can utilise the methods of nonlinear complex dynamics where characteristics of the motion in space and time, indicating the stability of the system behaviour, are computed in the reconstructed phase space from recorded ground motion. It will also facilitate the development of the data driven model(s) of rockmass dynamics close to the excavation faces.
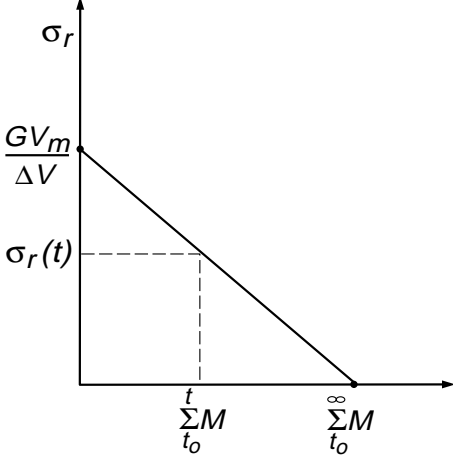
9.   Glossary of Terms

Parameter, relevant formula	Description
Magnitude, *m* $m = \log(A/T) + C$ *A/T* - the maximum displacement over associated period in the P- or S- wave group *C* - corrections for path effects, site response and source region	Magnitude is a relative measure of the strength of a seismic event based on measurements of maximum ground displacement at a given frequency at multiple seismic sites. A unit increase in magnitude corresponds to a 10-fold increase in amplitude of ground displacement. Gutenberg and Richter related seismic energy and magnitude derived from P-waves recorded at large distances from the source at 1sec period as $\log E(ergs) = 2.4m + 5.8$
Seismic moment, *M*, [Nm] and **Moment-magnitude**, *m* $m = 2/3 \log M - 6.1$	A scalar that measures the coseismic inelastic deformation at the source. Since seismic moment is proportional to the integral of the far field displacement pulse it can easily be derived from recorded waveforms. A relation that scales seismic moment into magnitude of a seismic event is called moment-magnitude.
Seismic moment tensor $M_{ij} = \int_V c_{ijkl}\, \Delta\epsilon_{kl}\, dV = \int_V \Delta\sigma_{ij}\, dV$, where c_{ijkl} - elastic constants $\Delta\epsilon_k$ - strain change at the source $\Delta\sigma_{ij}$ - stress change or change in moment per unit volume $\Delta\theta = tr\left(M_{ij}\right)/(3\lambda + 2G)$, where λ - the second Lamé constant *G* - rigidity	The most general description of the processes at the seismic source *V* is by the distribution of forces or moments equivalent to the inelastic deformation. One can describe the inelastic processes at the source as the stress-free change of size and shape of an elastic body without alteration of the elastic properties of the region. If change in size and shape can be expressed as a change in strain $\Delta\epsilon_{kl}$, then the equivalent stress change, or change in moment per unit volume is proportional to the strain change. The total moment integrated over the source volume is the seismic moment tensor, M_{ij}. For long waves compared to the source size, the whole source volume *V* can be considered to be a system of couples located at, say, the centre of *V*, and the moment tensor components can be defined by the equation at left. The moment tensor measures the inelastic deformation at the source during the seismic event and its value at the end of the source process measures the permanent inelastic strain produced by the event. The seismic moment tensor can be decomposed into isotropic (or volume change) and deviatoric components providing an additional insight into the nature of the coseismic strain drop. For a homogeneous body, the coseismic volumetric change, $\Delta\theta$, can be calculated from the second equation at left. The eigenvalues and corresponding eigenvectors of the deviatoric component of the seismic moment tensor describe the magnitude and orientation, respectively, of the principal moment axes (neglecting gravity) acting at the source. These principal moment axes are uniquely determined by moment tensor inversion. Principal moment orientation data can provide sufficient information to find the best stress tensor.
Radiated seismic energy, *E*, [J]	The portion of the energy released or work done at the source that is radiated as seismic waves. Seismic energy is proportional to the integral of the squared velocity spectrum in the far field and can be derived from recorded waveforms. Radiated seismic energy increases with stress drop, seismic moment and with the traction rate i.e., stress oscillations at the source.

Parameter, relevant formula	Description
Corner frequency, f_0, [Hz] and **Source size**, l, [m] $l = c_1 / f_0$ $c_1 \approx 2500$ for S-wave in hard rock	The frequency at which a source radiates the most seismic energy observed as the maximum on the source velocity spectrum or as the point at which a constant low frequency trend and a high frequency asymptote on the recorded source displacement spectrum intersect. The corner frequency is inversely proportional to the characteristic size of the source.
Stress drop, $\Delta\sigma$, [Pa] $\Delta\sigma = c_2 M f_o^3$ $c_2 \approx 1.8 \times 10^{-10}$ for S-waves in hard rock $\Delta\sigma = G\Delta\varepsilon$, and $\Delta\varepsilon$ - strain drop	Stress drop estimates the stress release at the seismic source. Although it is model dependent it provides reasonable estimates and a fair comparison amongst different sources from the same region recorded by the same seismic system.
Source area, [m^2] $A = M/(Gu)$ u - average displacement at the source.	The area of coseismic inelastic deformation over the planar source.
Source volume, [m^3] $V = M / \Delta\sigma$	The volume of coseismic inelastic deformation of the order of $\Delta\sigma/G$.
Apparent stress, [Pa] $\sigma_A = GE/M = E/(\Delta\varepsilon V)$ or $\sigma_A = E/(uA)$.	Apparent stress is recognised as a model independent measure of the stress change at the seismic source.
Apparent volume, [m^3] $V_A = M/(c_3\sigma_A) = M^2/(c_3 GE)$ c_3 - scaling factor ≈ 2.	The apparent volume scales the volume of rock with coseismic inelastic strain of an order of apparent stress over rigidity. The apparent volume V_A is less model dependent than the source volume V.
Energy index, EI	The notion of comparing the radiated energies of seismic events of similar moments can be translated into a practical tool called Energy Index (*EI*) – the ratio of the radiated energy of a given event (E) to the energy $\bar{E}(M)$ derived from the regional log$E$ vs log$M$ relation for a given moment M. Since $\log\bar{E}(M) = c + d\log M$, then $\bar{E}(M) = 10^{c+d\log M}$ where c and d are constant for a given ΔV and Δt. In general d-value increases with the system's stiffness and c, for a given d, increases with stress. A small or moderate event with $EI > 1$ suggests a higher than average shear stress at its location. The opposite applies to the $EI < 1$ case.
Seismic strain, $\varepsilon_s(\Delta V, \Delta t) = \Sigma M / (2G\Delta V)$ and **Seismic strain rate,** [s^{-1}] $\dot\varepsilon(\Delta V, \Delta t) = \varepsilon_s / \Delta t$	Seismic strain measures strain due to cumulative coseismic deformations within the volume ΔV over the period Δt. Its rate is measured by $\dot\varepsilon_s$.
Seismic stress, [Pa] $\sigma_s(\Delta V, \Delta t) = 2G\Sigma E / \Sigma M$	Seismic stress measures stress changes due to seismicity.
Seismic stiffness modulus, K_s [Pa] $K_s(\Delta V, \Delta t) = \sigma_s/\varepsilon_s = 4G^2\Delta V\Sigma E/(\Sigma M)^2$	Seismic stiffness measures the ability of the system to resist seismic deformation with increasing stress. The stiffer systems limit both the frequency and the magnitude of intermediate and large events but have time-of-day distribution with larger statistical dispersion, thus are less time predictable.

Parameter, relevant formula	Description
Seismic viscosity, [Pa · s] $\eta_s(\Delta V, \Delta t) = \sigma_s / \dot{\varepsilon}_s$	Seismic viscosity characterises the statistical properties of the seismic deformation process. Lower seismic viscosity implies easier flow of seismic inelastic deformation or greater stress transfer due to seismicity.
Seismic relaxation time, [s] $\tau_s(\Delta V, \Delta t) = \eta_s / G$	Seismic relaxation time quantifies the rate of change of seismic stress during seismic deformation processes and it separates the low frequency response from the high frequency response of the system under consideration. It also defines the usefulness of past data and the predictability of the flow of rock. The lower the relaxation time, the shorter the time span of useful past data and the less predictable the process of seismic deformation.
Seismic Deborah number $De_s(\Delta V, \Delta t) = \tau_s / flowtime$, where *flowtime* is a design parameter not necessarily equal to Δt.	Seismic Deborah number measures the ratio of elastic to viscous forces in the process of seismic deformation and has successfully been used as a criterion to delineate volumes of rockmass softened by seismic activity (soft clusters). The lower the Deborah number the less stable is the process or the structure over the design *flowtime* - what may be stable over a short period of time (large De_s) may not be stable over a longer time (lower De_s).
Seismic diffusivity, [m²/s] $D_s(\Delta V, \Delta t) = (\Delta V)^{2/3} / \tau_s$, or in a statistical sense $d_s = (\overline{X})^2 / \overline{t}$.	Seismic diffusivity can be used to quantify the magnitude, direction, velocity and acceleration of the migration of seismic activity and associated transfer of stresses in space and time. There is an inverse relationship between the diffusivity D_s and the friction parameters.
Seismic Schmidt number $Sc_{sD}(\Delta V, \Delta t) = \eta_s / (\rho D_s)$ or $Sc_{sd} = \eta_s / (\rho d_s)$ where ρ is rock density.	Seismic Schmidt number measures the degree of complexity in space and time (the degree of turbulence) of the seismic flow of rock. Note that seismic Schmidt number Sc_{sd}, encompasses all four independent parameters describing seismicity: $\overline{t}, \overline{X}, \Sigma M, \Sigma E$.
Time to failure, $(t_f - t)$ $d\Omega / dt = k / (t_f - t)^\alpha$ Ω - measurable quantity t - current time t_f - time of failure k, α - constants 	This concept describes the behaviour of materials in the terminal stages of failure. It views instability as a critical point, then precursors should follow characteristic power laws in which the rate of strain or other observable, measurable, quantity Ω is proportional to the inverse power of remaining time to failure. Observed oscillations in Ω of an increasing frequency as the failure approaches are part of the solution to time-to-failure equation with a complex exponent, where the imaginary part relates to discrete scale transformation and introduces log-periodic oscillations decorating the asymptotic power law. The observations Ω can be a combination of different seismic parameters that would exhibit power law type increase before failure. For well behaved data sets the time at failure t_f can be estimated from the times of three successive maxima (t_1, t_2, t_3) of the observed process $t_f = (t_2^2 - t_1 t_3) / (2t_2 - t_1 - t_3)$. Note that, in theory, $t_3 - t_2 < t_2 - t_1$

Parameter, relevant formula	Description
Seismic moments, volume mined and relative stress σ_r (vertical axis) $\dfrac{GV_m}{\Delta V}$ $\sigma_r(t)$ $\sum\limits_{t_0}^{t} M$ $\sum\limits_{t_0}^{\infty} M$ (horizontal axis)	If a volume of rock, V_m, is mined out at time t_0 and if the altered stress and strain field can readjust to an equilibrium state through seismic movements only, the sum of seismic moments released within a given period of time would be proportional to the excavation closure and in the long term at $t = t_\infty$ $$\sum_{t_0}^{\infty} M \simeq GV_m$$ where M is the scalar seismic moment. The relative stress level at the time, t, in a given volume of rock ΔV surrounding the excavation, can be calculated from the difference between GV_m and the cumulative moments released to date: $$\sigma_r(t) = (GV_m - \sum_{t_0}^{t} M)\,/\,\Delta V.$$
Seismic moments and volume of elastic convergence $\sum M = \gamma GV_e$	The amount of strain energy stored when mining in elastic rock is directly proportional to the volume of elastic convergence, V_e. It has been found that the total amount of seismic moment resulting from mining within a large area and time period is related to the change in elastic convergence V_e. The proportional constant gamma, γ, has been found to vary between about 0.03 and 1.0. There is some evidence that γ is a function of the geotechnical area being mined.

Acknowledgement

Bibliography

Books:
Aki, K and Richards, P. G. (1980). *Quantitative Seismology, Theory and Methods*. W. H. Freeman and Company, San Francisco.

Kostrov, B. V. and Das, S. (1988). *Principles of earthquake source mechanics.* Cambridge: Cambridge University Press.

Gibowicz, S. J. and Kijko, A. (1994). *An Introduction to Mining Seismology*. Academic Press, New York.

Mendecki, A. J., ed., (1997). *Seismic Monitoring in Mines*, Chapman and Hall, London.

Proceedings and periodicals:
Proceedings of the International Symposia on Rockbursts and Seismicity in Mines.
Bulletin of the Seismological Society of America.
Journal of Geophysical Research.
Geophysical Journal International.